

1 **Diffusion NMR Study of Complex Formation in**
2 **Membrane-Associated Peptides**

3 **Suliman Barhoum, Valerie Booth and Anand Yethiraj**

4
5 Received: date / Accepted: date

6 **Abstract** Pulsed-field-gradient nuclear magnetic resonance (PFG-NMR) is used to obtain
7 the true hydrodynamic size of complexes of peptides with sodium dodecyl sulfate SDS
8 micelles. The peptide used in this study is a 19-residue antimicrobial peptide, GAD-2. Two
9 smaller dipeptides, alanine-glycine (Ala-Gly) and tyrosine-leucine (Tyr-Leu), are used for
10 comparison. We use PFG-NMR to simultaneously measure diffusion coefficients of both
11 peptide and surfactant. These two inputs, as a function of SDS concentration, are then fit to
12 a simple two species model that neglects hydrodynamic interactions between complexes.
13 From this we obtain the fraction of free SDS, and the hydrodynamic size of complexes
14 in a GAD-2-SDS system as a function of SDS concentration. These results are compared
15 to those for smaller dipeptides and for peptide-free solutions. At low SDS concentrations
16 ($[\text{SDS}] \leq 25 \text{ mM}$), the results self-consistently point to a GAD-2-SDS complex of fixed
17 hydrodynamic size $R = (5.5 \pm 0.3) \text{ nm}$. At intermediate SDS concentrations ($25 \text{ mM} < [\text{SDS}]$)

Suliman Barhoum
Department of Physics and Physical Oceanography, Memorial University of Newfoundland, St. John's, NL,
Canada
E-mail: sulimanb@mun.ca,
Valerie Booth
Department of Biochemistry, Memorial University of Newfoundland, St. John's, NL, Canada
Tel.: 709-864-4523
E-mail: vbooth@mun.ca,
Anand Yethiraj
Department of Physics and Physical Oceanography, Memorial University of Newfoundland, St. John's, NL,
Canada
Tel.: 709-864-2113
E-mail: ayethiraj@mun.ca

18 < 60 mM), the apparent size of a GAD-2-SDS complex shows almost a factor of two increase
19 without a significant change in surfactant-to-peptide ratio within a complex, most likely
20 implying an increase in the number of peptides in a complex. For peptide-free solutions,
21 the self-diffusion coefficients of SDS with and without buffer are significantly different at
22 low SDS concentrations but merge above [SDS]=60 mM. We find that in order to obtain
23 unambiguous information about the hydrodynamic size of a peptide-surfactant complex
24 from diffusion measurements, experiments must be carried out at or below [SDS] = 25 mM.

25 **Keywords** Antimicrobial peptide · Peptide-micelle complexes · NMR diffusometry

26 **Introduction**

27 Membrane-associated proteins and peptides are often studied in a micellar environment
28 (Tulumello and Deber, 2009; Sanders and Sönnichsen, 2006). Like membrane bilayers, mi-
29 celles provide a hydrophobic-hydrophilic interface, but unlike them, they are small enough
30 to enable solution NMR signals to be observed. Micelles are commonly employed in NMR
31 structure determination of membrane proteins (Qureshi and Goto, 2012; Tulumello and
32 Deber, 2009), but have also been used in studies where the protein-lipid interaction itself is
33 the focus (Cozzolino et al, 2008; Morein et al, 1996; Yu et al, 2006; Romani et al, 2010). NMR-
34 based techniques have been utilized to study an important class of membrane-associated
35 proteins that are called antimicrobial peptides (AMPs).

36 AMPs are often short peptides consisting of 12 to 50 residues and act by interacting
37 with (and often disrupting) membranes. AMPs have been shown to play an important
38 role in attacking and killing microbes such as bacteria, viruses, and fungi (Zasloff, 2002;
39 Nicolas, 2009; Hoskin and Ramamoorthy, 2008; Chinchar et al, 2004). Moreover, some AMPs
40 exhibit activity against tumor cells in a mammal's body by disrupting the membrane of the
41 diseased cells and targeting the cell interior without affecting the membrane of host cells
42 (Rege et al, 2007). This selectivity, for microbial and/or tumor cells, is thought to arise due
43 to the amphiphilic structure of the AMP that has an affinity to the lipid bilayer structure of
44 the microbial cells as well as due to the interaction between the positive charge on the AMP

45 with the anionic components of the tumor or pathogen cell membrane (Eband and Vogel,
46 1999). Therefore, anionic sodium dodecyl sulfate SDS surfactant micelles are commonly
47 employed in the structural studies of AMPs, as well as other membrane proteins (Wang,
48 2008, 1999; Whitehead et al, 2001; Orfi et al, 1998; Begotka et al, 2006; Deaton et al, 2001;
49 Whitehead et al, 2004; Gao and Wong, 1998; Buchko et al, 1998).

50 A knowledge of the hydrodynamic size of proteins plays an important role in un-
51 derstanding their conformations (Jones et al, 1997). This is also the case for peptides in
52 peptide-micelle complexes, where there could be many coexisting conformations. The hy-
53 drodynamic size of complexes can be obtained by measuring diffusion coefficients and
54 using the Stokes-Einstein-Sutherland equation $R_H = K_B T / 6\pi\eta D_o$. This approach, however,
55 is only strictly valid when the self-diffusion coefficient D_o is obtained by measuring the
56 diffusion coefficient as a function of the surfactant concentration and then extrapolating to
57 infinite dilution. Such a procedure is often not practical when the amount of peptide or pro-
58 tein is limited in quantity. As a result of this, “apparent” hydrodynamic radii are routinely
59 reported, without such extrapolation, in systems with rather large surfactant concentrations
60 (Binks et al, 1989; Gimel and Brown, 1996; Sarker et al, 2011).

61 An important phenomenon to consider with respect to large macromolecular concen-
62 trations is crowding. Macromolecular crowding usually refers to the non-specific excluded
63 volume (steric) effect of macromolecules with respect to one another in an environment
64 where the macromolecular volume fraction Φ is large; an example is a living cell with
65 $\Phi=40\%$ (Zhou et al, 2008). At finite dilutions there are hydrodynamic corrections to dif-
66 fusion (Batchelor, 1976) even for a simple colloidal system of spherical particles. In the
67 literature, crowding has long been treated as an excluded volume interaction at high vol-
68 ume fractions. It is now being realized that electrostatic and hydrodynamic interactions
69 sensitively affect macromolecular dynamics (Zhou et al, 2008; Schreiber et al, 2009). As a
70 result, crowding-related effects can be important even at relatively low volume fractions.
71 For example, for a micelle of radius 2 nm in a solution with Debye length $\kappa^{-1} = 1$ nm, the
72 effective radius is 3 nm and $\Phi=10\%$ corresponds to $\Phi_{\text{eff}} \approx 34\%$, which already represents a
73 relatively dense colloidal regime. Thus, we generalize macromolecular crowding to refer to

74 all concentrations where excluded volume, electrostatic or hydrodynamic interactions are
75 at play.

76 The nature of the association of peptides with anionic SDS micelles depends on the
77 details of the electrostatic environment; for example, cationic peptides bind more strongly
78 than their zwitterionic counterparts (Begotka et al, 2006). NMR diffusometry studies have
79 found that peptide binding with anionic SDS micelles and zwitterionic dodecylphospho-
80 choline (DPC) micelles are different, also due to the difference in electrostatic environment
81 (Whitehead et al, 2004). Similarly, it was found that a cell-penetrating peptide (CPP) al-
82 ters the dynamics and size of neutral and negatively charged bicelles in different ways
83 (Andersson et al, 2004).

84 PFG-NMR studies have shown that the hydrophobic interaction can play a signifi-
85 cant role on the binding of peptides and tripeptides to micelles (Deaton et al, 2001; Orfi
86 et al, 1998), as well as neuropeptides to a membrane-mimic environment (Chatterjee et al,
87 2004). NMR studies were also carried out to explore the binding of a neuropeptide to
88 SDS micelles in the presence of zwitterionic 3-[(3-cholamidopropyl) dimethylammonio]-
89 1-propanesulfonate (CHAPS) surfactant as a crude model for cholesterol in the biological
90 membrane. These studies showed that having comicelles composed of SDS and CHAPS sur-
91 factants inhibits the hydrophobic interaction of the neuropeptide with the core of comicelles
92 (Whitehead et al, 2001).

93 Since AMPs are subjects of much interest and also represent an even larger class of
94 amphipathic, helical peptides, the peptide, GAD-2 with a 19-amino acid sequence (FLH-
95 HIVGLIHHGLSLFGDR), was selected for this study. GAD-2 and a related peptide, GAD-1
96 with a 21-amino acid sequence, have been identified in recent efforts to discover new AMPs
97 (Fernandes et al, 2010; Browne et al, 2011; Ruangsri et al, 2012). GAD-2 has recently been
98 shown by NMR and circular dichroism to take on a helical structure in SDS micelles at 40°
99 C, although it loses a certain amount of its helicity at room temperature (unpublished data).
100 While the GAD-2 -SDS peptide-micelle system chosen is relevant and of current interest
101 in biochemical studies, the goal of this study was to provide a realistic picture of complex
102 formation in peptide-micelle systems in general.

103 In this work, we used NMR diffusometry to study the interaction between the cationic
104 GAD-2 AMP and an anionic SDS micelle as a membrane mimic environment. In order to do
105 so, we use a simple mathematical model that is utilized to signal the changes in the nature of
106 the macromolecular complexes in a system of nonionic polymer-anionic surfactant system
107 in aqueous solution (Barhoum and Yethiraj, 2010). Similar models, based on fast exchange
108 between two or more sites, have been employed previously in surfactant (Stilbs, 1982,
109 1983) and peptide-surfactant systems (Chen et al, 1995; Deaton et al, 2001) and utilized in
110 the latter to extract peptide-micelle binding characteristics. We compare the nature of the
111 resulting peptide-SDS complex with those that form with two much smaller peptides, and
112 are able to identify important distinguishing characteristics. We find, reassuringly, that the
113 most minimal model to extract hydrodynamic size works well for peptides, at least for
114 those with the size (19 residues) of GAD-2; however, one must be careful to avoid the onset
115 of crowding in order to reliably use these simple models.

116 **1 Materials and Methods**

117 GAD-2 peptide with average molecular mass $M_w=2168$ g/mole was synthesized using solid
118 phase chemical synthesis employing O-fluorenylmethoxycarbonyl (Fmoc) chemistry, on
119 a CS336X peptide synthesizer (C S Bio Company, Menlo Park, CA) following the man-
120 ufacturer's instructions. The peptides were synthesized at a 0.2 mmol scale with a single
121 coupling, using prederivatized Rink amide resin. Resin and all Fmoc amino acids were pur-
122 chased from C S Bio Company Organic solvents and other reagents used for the synthesis
123 and purification were high- performance liquid chromatography (HPLC) grade or better
124 and purchased from Fisher Scientific (Ottawa, ON) and Sigma-Aldrich Canada (St. Louis,
125 MO). Deprotection and cleavage of the peptides from the resin were conducted with a
126 trifluoroacetic acid (TFA)/water (95:5 by volume) cleavage cocktail followed by cold precip-
127 itation with tert-butyl ether. The crude products were purified by preparative reverse-phase
128 HPLC in a Vydac C-8 column by use of a water/acetonitrile linear gradient with 0.1% TFA
129 as the ion pairing agent. The molecular weights of the peptides were confirmed by matrix-

130 assisted laser desorption ionization time of flight (MALDI-TOF) mass spectrometry. The
 131 purified peptides were lyophilized and stored at 4 °C.

132 Ala-Gly peptide with $M_w=146.14$ g/mole, Tyr-Leu peptide with $M_w=294.35$ g/mole, and
 133 SDS (99% purity) with $M_w=288.38$ g/mole were purchased from Sigma-Aldrich Canada
 134 (St. Louis, MO) and were used as received without further purification. Deuterium oxide
 135 D_2O with 99.9% isotopic purity was purchased from Cambridge Isotope Laboratories (St.
 136 Leonard, Quebec).

Table 1 Sample nomenclature. All samples were made with D_2O as a solvent, and unless stated have 0.1 M sodium oxalate buffer in them. Final concentrations [SDS] were achieved by mixing different stock solutions. The molar ratio $R = [\text{peptide}]/[\text{SDS}] = 30$ was kept constant for GAD-2 solutions.

Abbreviation	Final [SDS]
SDS-buf	2-187 mM
GAD-2-SDS	1-80 mM
Ala-Gly-SDS	2-60 mM
Tyr-Leu-SDS	2-60 mM

137 GAD-2-SDS, Ala-Gly-SDS, Tyr-Leu-SDS, and SDS samples were prepared with compo-
 138 sitions according to table 1. The molar ratio (R) of SDS concentration to peptide concentra-
 139 tion in GAD-2-SDS samples was held constant ($R = [\text{SDS}]/[\text{GAD-2}] = 30$). The concentration
 140 of dipeptides (Ala-Gly and Tyr-Leu) in Ala-Gly-SDS and Tyr-Leu-SDS systems was 2 mM.
 141 The pH value for all samples was adjusted to be 4 by the addition of sodium deuterioxide
 142 or deuterium chloride. All samples were made with D_2O as solvent and, unless otherwise
 143 stated, have 0.1 M sodium oxalate buffer ($Na_2C_2O_4$) in them. Sodium oxalate buffer was
 144 used in previous NMR studies to adjust the pH of SDS micelle-peptide solutions (Orfi et al,
 145 1998; Deaton et al, 2001). It is effective as a buffer for pH below 5, where the histidine-rich
 146 GAD-2 peptide is expected to have a net positive charge. Moreover, the chemical structure
 147 of sodium oxalate does not include protons in it. As a result, the one dimensional proton
 148 NMR spectra do not include buffer peaks that might overlap with SDS and peptides peaks.

149 The self-diffusion measurements were carried out in a diffusion probe (Diff30) and with
 150 maximum field gradient 1800 G/cm (applied along the z-axis) at a resonance frequency of
 151 600 MHz on a Bruker Avance II spectrometer. The maximum gradient used in this work was

152 300 G/cm. Diffusion was measured with a pulsed-field gradient stimulated-echo sequence
153 (Price, 1997) with (almost square) trapezoidal gradient pulses. The diffusion coefficient of
154 a molecule in aqueous solution is obtained from the attenuation of the signal according to
155 the equation (Price, 1997)

$$\ln\left(\frac{S(k)}{S(0)}\right) = -Dk \quad (1)$$

156 where $S(k)$ is the "intensity" of the signal (the integration of the relevant peak region)
157 in the presence of field gradient pulse, $S(0)$ is the intensity of the signal in the absence
158 of field gradient pulse, $k = (\gamma\delta g)^2(\Delta - \delta/3)$ is a generalized gradient strength parameter,
159 $\gamma = \gamma^H = 2.6571 \times 10^8 \text{ T}^{-1}\text{s}^{-1}$ is the gyromagnetic ratio of the ^1H nucleus, $\delta = 2 \text{ ms}$ is the
160 duration of the field gradient pulse, $\Delta = 100 \text{ ms}$ is the time period between the two field
161 gradient pulses, and g is the amplitude of the field gradient pulse.

162 2 Results and Discussion

163 Complementary NMR-based techniques were utilized in order to identify components for
164 different samples based on their one-dimensional NMR spectra and to extract parameters
165 such as self-diffusion coefficients. The one-dimensional (1D) proton NMR spectra at a reso-
166 nance frequency of 600 MHz on a Bruker Avance II spectrometer and at sample temperature
167 298 K are shown in figure 1. In all cases the trace signal of HDO in D_2O is the most dominant
168 peak (at $\approx 4.7 \text{ ppm}$); however the HDO, peptide and SDS peaks are all spectrally separable.
169 In NMR, chemical shifts can be utilized to provide informatoin about the structure and
170 the change in the chemical environment of molecules. For example, it was found (Morris
171 et al, 2005) that both the chemical shift and the observed diffusion coefficient are affected
172 by complexation. However, in our work, we specifically prepared our samples so that the
173 SDS concentration was varied, but with the molar ratio $R = [\text{SDS}]/[\text{GAD-2}]$ held constant.
174 We thus do not see a change in either linewidths or chemical shifts as a function of SDS
175 concentration.

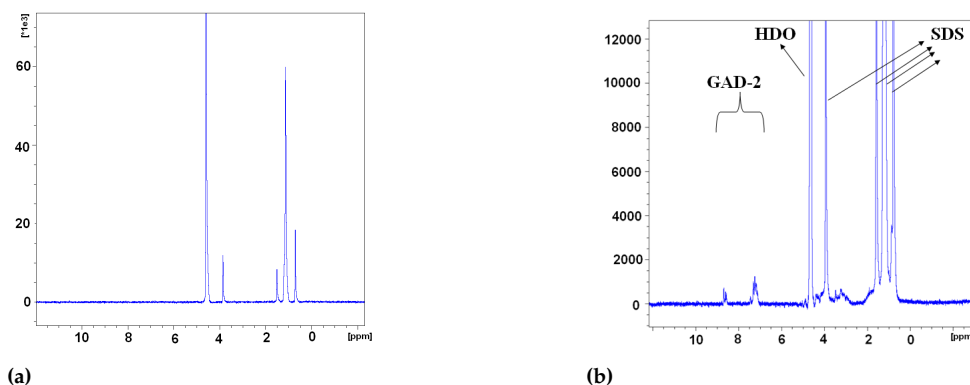


Fig. 1 1D ^1H NMR spectrum for (a) a peptide-free SDS sample with $[\text{SDS}] = 6 \text{ mM}$ (b) a GAD-2-SDS sample with $[\text{SDS}] = 60 \text{ mM}$ and $[\text{GAD-2}] = 2 \text{ mM}$. Sample temperature is 298 K.

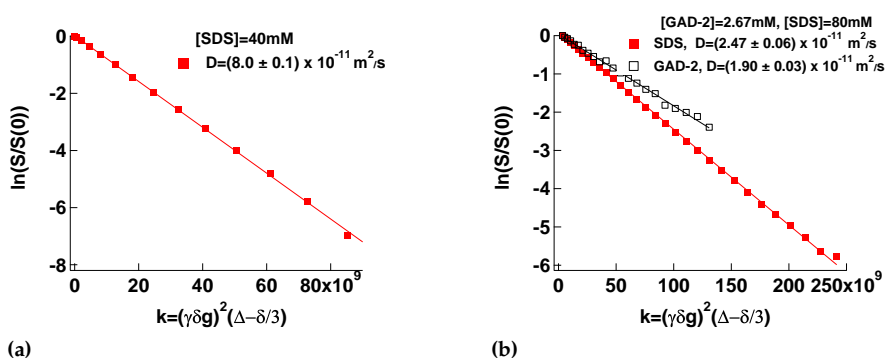


Fig. 2 The attenuation of the signal $S(k)/S(0)$ on a log scale versus $k = (\gamma\delta g)^2(\Delta - \delta/3)$ for (a) a peptide-free SDS sample with $[\text{SDS}] = 40 \text{ mM}$ and 0.1 M sodium oxalate buffer (b) a GAD-2-SDS sample with $[\text{SDS}] = 80 \text{ mM}$, $[\text{GAD-2}] = 2.67 \text{ mM}$, and 0.1 M sodium oxalate buffer. $\delta = 2 \text{ ms}$ and $\Delta = 100 \text{ ms}$. The errors in the values of the diffusion coefficients represent the uncertainty in the slope obtained from a linear fit to $\ln(S/S_0)$ vs k . Typical values of R^2 are of order 0.998.

176 In this work, we carried out experiments with peptide at varying SDS concentrations
 177 in the presence of sodium oxalate buffer. We also performed experiments on pure SDS
 178 solutions as well as buffered SDS solutions for comparison. Figure 2 shows the signal at-
 179 tenuation and the self-diffusion coefficients for SDS and peptides in a buffered peptide-free
 180 SDS sample and GAD-2-SDS sample. The signal attenuation in all samples was observed
 181 to be monoexponential.

182 This suggests that the exchange of SDS molecules between the SDS in micelles and
 183 in free solution must be very rapid in the NMR time scale. The values of the observed

184 diffusion coefficients were calculated from the monoexponential decays using equation 1.
185 For peptide-free SDS solutions prepared with sodium oxalate buffer (figure 2a), the signal
186 attenuation of SDS was obtained by integrating the area under the spectral region between
187 0 to 4 ppm. For the GAD-2-SDS system, the spectral ranges from 0 to 4 ppm and 7 to 9 ppm
188 were used to obtain SDS and GAD-2 signal attenuation, respectively. In each case the SDS
189 and peptide spectral regions were chosen to ensure a clear spectral separation.

190 2.1 Diffusometry

191 2.1.1 Surfactant Solutions and Analysis Methods

192 Figure 3a shows the self-diffusion coefficient of SDS in 3 peptide-free SDS systems: one with
193 sodium oxalate buffer with pH=4 (red open circles), and two without sodium oxalate buffer.
194 Of the unbuffered solutions one was with pH unadjusted but measured to be between 3
195 and 3.5 (blue open squares), and one with the pH=4 (black filled squares). Below [SDS]
196 = 60 mM, the SDS diffusion coefficient D_{Obs}^{SDS} for unbuffered solutions at different pH are
197 indistinguishable from each other, while values in the buffered solution are much lower.

198 The pulsed-field-gradient signal attenuation is monoexponential for all samples (fig-
199 ure 2). This implies that the exchange of SDS molecules between the SDS in micelles and
200 in free solution is rapid in the NMR time scale. Previous studies (Soderman and Stilbs,
201 1994; Stilbs, 1982, 1983) showed that a surfactant molecule visits more than one environ-
202 ment over very short timescales, and interpreted the observed diffusion coefficients using a
203 two-site exchange model. In all the systems considered here, the SDS surfactant can either
204 be a free monomer in solution or associated with a surfactant-rich aggregate. The observed
205 self-diffusion coefficient of SDS is thus a linear combination of the self-diffusion coefficient
206 D_{free}^{SDS} of the free molecules in bulk and that of the bound molecules in the micelle $D_{micelle}^{SDS}$ in
207 peptide-free solutions or a peptide-SDS complex D_{Aggr}^{SDS}

$$\begin{aligned}
 D_{\text{Obs}}^{\text{SDS}} &= D_{\text{free}}^{\text{SDS}}, & [\text{SDS}] &\leq C_0, \\
 D_{\text{Obs}}^{\text{SDS}} &= (D_{\text{free}}^{\text{SDS}} - D_{\text{Aggr}}^{\text{SDS}})(f_s) + D_{\text{Aggr}}^{\text{SDS}}, & [\text{SDS}] &> C_0
 \end{aligned} \tag{2}$$

208 where $f_s = [\text{SDS}]_{\text{free}}/[\text{SDS}]$ is the fraction of free SDS molecules, $D_{\text{Aggr}}^{\text{SDS}}$ is either the micellar
 209 diffusion coefficient in peptide-free samples, or the diffusion coefficient of the micelle-
 210 peptide complex, and C_0 refers to the critical (micellar or aggregation) concentration (CMC
 211 or CAC), and $[\text{SDS}]$ is the total SDS concentration. A key assumption of the model is that
 212 there are only two distinct species, the free and the aggregate states; however, as will be
 seen later, we are able to check for self-consistency of the model.

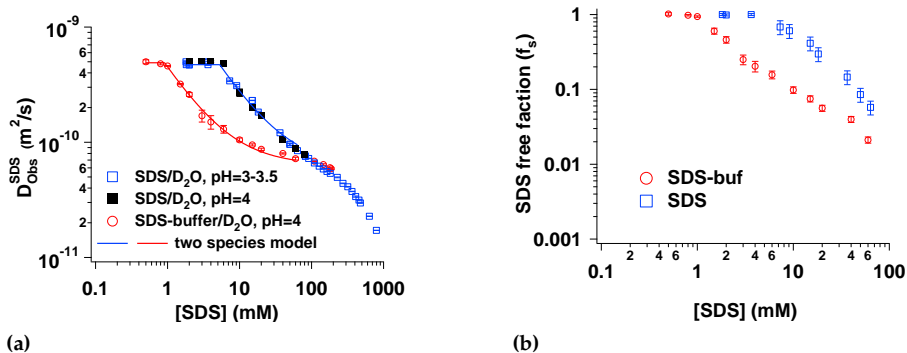


Fig. 3 Self-diffusion coefficient in peptide-free SDS solutions. (a) D versus SDS concentration $[\text{SDS}]$ for solutions with sodium oxalate buffer (pH=4) (red open circles), and unbuffered, with pH=3-3.5 (blue open squares), and with pH=4 (black filled squares). (b) Fraction (f_s) of free SDS with and without sodium oxalate buffer.

213

214 For simple spherical micelle systems, buffered and unbuffered peptide-free SDS solu-
 215 tions, $[\text{SDS}]_{\text{free}} = \text{CMC}$ for $[\text{SDS}] > \text{CMC}$. Therefore, equation 2 has 3 parameters, $C_0 = \text{CMC}$,

216 $D_{\text{free}}^{\text{SDS}}$ and $D_{\text{micelle}}^{\text{SDS}}$. Fitting the buffered peptide-free SDS solution to the two-species model
 217 in equation 2 yields the parameters $D_{\text{free}}^{\text{SDS}} = (4.90 \pm 0.07) \times 10^{-10} \text{ m}^2/\text{s}$, $D_{\text{micelle}}^{\text{SDS}} = (6.3 \pm 0.4)$
 218 $\times 10^{-11} \text{ m}^2/\text{s}$, and $\text{CMC} = (0.91 \pm 0.02) \text{ mM}$, while for the unbuffered peptide-free SDS solu-

219 tion $D_{\text{free}}^{\text{SDS}} = (4.71 \pm 0.08) \times 10^{-10} \text{ m}^2/\text{s}$, $D_{\text{micelle}}^{\text{SDS}} = (6.1 \pm 0.9) \times 10^{-11} \text{ m}^2/\text{s}$, and $\text{CMC} = (5.3 \pm 0.2) \text{ mM}$.

220 The main physical insight hidden in these curves is the onset of crowding. While the
 221 unbuffered and buffered solutions have very different dynamics at low [SDS], they both
 222 report a constant and similar micelle size upto 60 mM. Above 60 mM, the observed diffu-
 223 sion is reporting on micellar diffusion in an environment where inter-micellar interactions
 224 cannot be neglected. Two effects are thus inseparable in either dynamic light scattering or
 225 pulsed-field-gradient NMR: reduction in micellar diffusion coefficient due to increase in hy-
 226 drodynamic size, and increase in hydrodynamic interactions between complexes. Such an
 227 effect of hydrodynamic interactions has indeed been previously noted (Ando and Skolnick,
 228 2010).

229 2.1.2 Peptide: GAD-2

230 When the size of a hydrophobic peptide is large enough that surfactant motion is rapid
 231 on the timescale of peptide motion, the peptide is expected to be associated with several
 232 surfactant molecules and there should never be free peptide, i.e. the peptide binding fraction
 233 is close to 1. For example, in the GAD-2–SDS system, since the concentration of SDS is 30
 234 times higher than GAD-2 concentration ($R = [\text{SDS}]/[\text{GAD} - 2] = 30$), we know that there is
 235 unlikely to be free peptide: we will test this assumption soon.

In this case, $D_{\text{Aggr}}^{\text{SDS}} = D_{\text{Aggr}}^{\text{Peptide}} \approx D^{\text{Peptide}}$. Using this additional information allows us to use the two-site model even if the $D_{\text{Obs}}^{\text{SDS}}$ versus $1/[\text{SDS}]$ relationship is not linear. The only proviso is that the overall particulate volume fraction must always be small enough that hydrodynamic effects are negligible. For the peptide-free SDS system, we have seen that this is generally true for concentrations below 60 mM, or volume fractions below 0.04. For GAD-2–SDS system, the size of an GAD-2–SDS aggregate is expected to change with SDS concentration. Therefore, the concentration $[\text{SDS}]_{\text{free}}$ of free SDS monomers is expected to change in the SDS concentration regime above CAC. We may simply rewrite and rearrange equation 2 for $[\text{SDS}] > C_0$ but with $D_{\text{Aggr}}^{\text{SDS}} = D^{\text{Peptide}}$,

$$f_s([\text{SDS}]) = \frac{[\text{SDS}]_{\text{free}}}{[\text{SDS}]} = \frac{D_{\text{Obs}}^{\text{SDS}} - D^{\text{Peptide}}}{D_{\text{free}}^{\text{SDS}} - D^{\text{Peptide}}}. \quad (3)$$

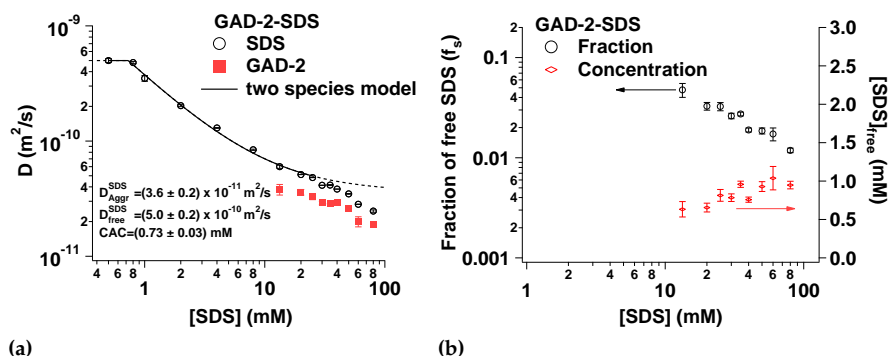


Fig. 4 (a) Self-diffusion coefficient of GAD-2 and SDS in a GAD-2-SDS system with $R=[\text{SDS}]/[\text{GAD-2}]=30$ versus SDS concentration [SDS] (b) Fraction (f_s) of free SDS and concentration ($[\text{SDS}]_{\text{free}}$) of free SDS versus SDS concentration [SDS]

236 Figure 4a shows the self-diffusion coefficient of GAD-2 and SDS in the GAD-2-SDS
 237 system. We measured the self-diffusion of GAD-2 in the SDS concentration range that is
 238 higher than 13.3 mM. Due to experimental limitations (small value of signal-to-noise ratio),
 239 we were not able to extract the self-diffusion coefficient of GAD-2 in the SDS concentration
 240 range below 13.3 mM, but we were able to measure the surfactant diffusion.

241 The SDS self diffusion coefficient is fit well to the two species model for $[\text{SDS}] \leq 25$
 242 mM (figure 4a, solid line), and it deviates from the fit for higher SDS concentration (fig-
 243 ure 4a, dotted line). The resulting fit parameters are $D_{\text{free}}^{\text{SDS}} = (5.0 \pm 0.2) \times 10^{-10} \text{ m}^2/\text{s}$, $D_{\text{Aggr}}^{\text{SDS}}$
 244 $= (3.6 \pm 0.2) \times 10^{-11} \text{ m}^2/\text{s}$, and $CAC = (0.73 \pm 0.03) \text{ mM}$. We now test the assumption that
 245 there is no free peptide. Using a two-site exchange model similar to Equation 2, but for the
 246 peptide (with $D_{\text{Obs}}^{\text{Peptide}} = 3.8 \times 10^{-11} \text{ m}^2/\text{s}$ at $[\text{SDS}] = 13 \text{ mM}$ and $D_{\text{free}}^{\text{Peptide}} \geq 1.6 \times 10^{-10} \text{ m}^2/\text{s}$,
 247 the value in SDS-free buffered peptide system at $[\text{GAD-2}] = 2 \text{ mM}$, and $D_{\text{Aggr}}^{\text{Peptide}} = D_{\text{Aggr}}^{\text{SDS}}$), we
 248 calculated the fraction of free peptide at $[\text{SDS}] = 13 \text{ mM}$ to be $\leq 1.6\%$. Previous studies (Gao
 249 and Wong, 1998) reported the partitioning of adrenocorticotrophic hormone (ACTH) pep-
 250 tides in SDS and DPC micelles. There too, the fraction of ACTH bound to SDS is over
 251 99%.

252 PFG-NMR can be used to get spectrally-resolved diffusion coefficients (Morris and
 253 Johnson, 1992; Morns and Johnson, 1993; Hinton and Johnson, 1994; Wu et al, 1994; Altieri

254 et al, 1995). Using both SDS and peptide diffusion coefficients as a function of [SDS], we
 255 extract the fraction (f_s) of free surfactant in the monomer state in the aqueous solution
 256 as well as the concentration of free surfactant $[\text{SDS}]_{\text{free}}$. This is shown in figure 4b. With
 257 increasing surfactant concentration, f_s decreases while $[\text{SDS}]_{\text{free}}$ rises from 0.7 mM (close to
 258 the CAC) to ≈ 1 mM (close to the CMC). This is consistent with the picture (Barhoum and
 259 Yethiraj, 2010; Jones, 2002) that the concentration of free surfactant above the CAC/CMC is
 260 equal to the value of the CAC/CMC. In the peptide-SDS system, and similar to the behavior
 261 in the nonionic polymer–anionic surfactant (poly(ethylene)oxide–SDS) system (Barhoum
 262 and Yethiraj, 2010), the free concentration rises further until it reaches the CMC value in
 263 the buffered solution.

Next, we estimate the hydrodynamic radius R_H of GAD-2–SDS complexes (figure 5a)
 using the Sutherland – Stokes – Einstein equation (Jones, 2002)

$$R_H = \frac{K_B T}{6\pi\eta D} \quad (4)$$

264 where K_B is the Boltzmann constant, T is the absolute temperature, and η is the solvent
 265 viscosity ($\eta_{D_2O}=1.1$ mPa.s). The hydrodynamic radius R_H is obtained from the peptide
 266 diffusion ($D = D^{\text{Peptide}}$, open squares in figure 5a) as well as from the fitted value of $D_{\text{Aggr}}^{\text{SDS}}$
 267 obtained from the concentration dependence of the surfactant diffusion (dashed red line
 268 in figure 5a). For $[\text{SDS}] < 25$ mM the hydrodynamic radii obtained via peptide diffusion
 269 and surfactant diffusion are roughly the same, with a value of approximately 5.5 nm.
 270 Interestingly, R_H (obtained from peptide diffusion D^{Peptide}) increases as a function of SDS
 271 concentration to about 10 nm at 60 mM, less than a factor of two increase.

272 Plotted in figure 5b is the variation in the ratio of SDS molecules to peptide molecules in
 273 a complex $r = ([\text{SDS}] - [\text{SDS}]_{\text{free}})/([\text{SDS}]/R) = (1 - f_s) R$ exhibits a very slight increase, from
 274 ≈ 28 to 29, and approaches $R = 30$ asymptotically. We need to understand how the aggregate
 275 size changes in order to accommodate the two-fold increase in the hydrodynamic radius
 276 R_H ; we will return to this point later.

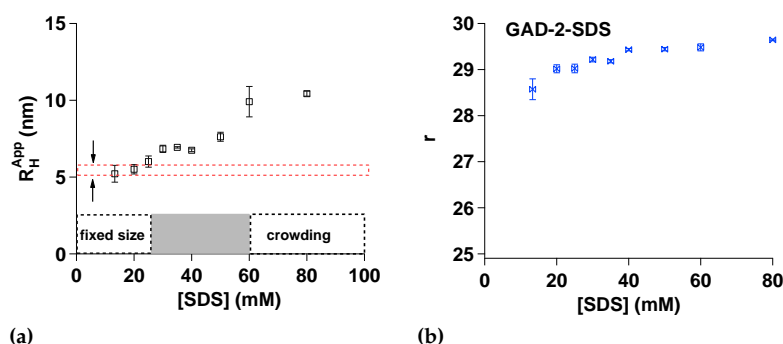


Fig. 5 (a) The apparent hydrodynamic radius (R_H^{APP}), extracted from the peptide diffusion coefficient, of GAD-2-SDS complexes versus SDS concentration [SDS]. The horizontal dashed line is the value of apparent hydrodynamic radius ($R_H^{APP} = 5.5 \pm 0.3$ nm) obtained *via* the SDS aggregate diffusion coefficient ($D_{Aggr}^{SDS} = (3.6 \pm 0.2) \times 10^{-11}$ m²/s) at low SDS concentration [SDS] ≤ 25 mM, where the two species model is valid. This value is in agreement with the peptide diffusion coefficient. At high SDS concentration [SDS] ≥ 60 mM. The diffusion coefficient measured gives no information about the true hydrodynamic radius. The intermediate SDS concentration regime, denoted by the gray area, is the regime in which either complex size is indeed increasing with concentration or hydrodynamic interactions between complexes is slowing down the motions. (b) The ratio of SDS molecules to peptide molecules in a complex (r) versus SDS concentration ([SDS]) for GAD-2-SDS samples.

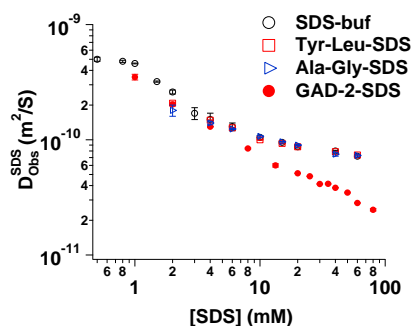


Fig. 6 Self-diffusion coefficient of SDS in all the systems studied: peptide-free SDS system with sodium oxalate buffer, Tyr-Leu-SDS, Ala-Gly-SDS, and GAD-2-SDS with $R=[SDS]/[GAD-2]=30$ samples.

277 2.1.3 Comparison with smaller dipeptides

278 In order to study the effect of peptide size on the dynamics of peptide-SDS complexes, and to
 279 ensure consistency with previous work on small peptides (Deaton et al, 2001), diffusometry
 280 was carried out to quantify complex formation of SDS with the dipeptides Ala-Gly and
 281 Tyr-Leu. The measured diffusion coefficients for both the SDS and peptides are consistent
 282 with those measured at one SDS concentration in that previous work (Deaton et al, 2001).

283 A plot of the SDS self-diffusion coefficient for all systems in the current study in one
284 graph (figure 6) shows clearly that SDS diffusion looks similar for the systems with small
285 di-peptides (Ala-Gly and Tyr-Leu) and the peptide-free SDS system with sodium oxalate
286 buffer. This suggests that the fraction of free SDS in the Tyr-Leu-SDS and Ala-Gly-SDS
287 systems is similar to the fraction of free SDS in the peptide-free SDS system with buffer
288 (figure 3b). On the other hand, SDS diffusion looks very different for the system with long
289 peptide (GAD-2-SDS system), suggesting that the GAD-2-SDS complexes are very different
290 from the Ala-Gly-SDS and Tyr-Leu-SDS complexes, which are essentially indistinguishable
291 from micellar aggregates with no peptide.

292 This means that the peptide-micelle binding characteristics of the Tyr-Leu and Ala-Gly
293 dipeptides are different from the much longer GAD-2 peptide. Also, this indicates that
294 GAD-2 significantly disrupts the micellar aggregate. This conclusion likely extends to other
295 long and hydrophobic peptides.

296 3 Conclusion

297 NMR-based techniques have been utilized in this work to study the nature of peptide-
298 micelle complexes in a buffered 19-residue antimicrobial peptide (the GAD-2-SDS system).
299 First, we examined the impact of the buffer (figure 3a). Varying the pH over a small range in
300 the absence of a buffer shows no effect on the micellar structure, while the CMC is lower in
301 the presence of the buffer. The addition of sodium salts more effectively screens the charge on
302 the micelle. In other work it has been found to result in larger stable micelles (Sammalkorpi
303 et al, 2009; Berr and Jones, 1988) and lower critical micellar concentrations (Iyota and
304 Krastev, 2009).

305 For pure (peptide-free) SDS solutions, the observed diffusion coefficients of surfactant
306 SDS molecules for buffered and unbuffered solutions merge at surfactant concentrations
307 $[SDS] > 60$ mM. In addition, the linear two species model (equation 2) is robustly valid
308 below $[SDS]=60$ mM, with micelle size being independent of SDS concentration. This is
309 similar to the findings in previous work for a system of anionic surfactant (SDS)-nonionic

310 polymer polyethylene oxide (PEO) (Barhoum and Yethiraj, 2010) where this concentration
 311 was identified as the onset of macromolecular crowding: this refers to the excluded volume
 312 effect of one macromolecule with respect to another (Zhou et al, 2008). Our primary finding
 313 is that [SDS]=60 mM signals the concentration beyond which one cannot, even in principle,
 314 extract hydrodynamic radii or aggregate ratios.

315 At low surfactant concentrations ([SDS] < 25 mM), the observed diffusion coefficient of
 316 SDS (figure 4a) is well described by the two-species model in equation 2, with both monomer
 317 and aggregate having a size that does not depend on SDS concentration. Moreover, in this
 318 range, the surfactant aggregate diffusion coefficient and the peptide diffusion coefficient
 319 coincide. This is a self-consistency check that gives confidence in the linear two species
 320 model and the results obtained.

321 At intermediate SDS concentrations, the apparent hydrodynamic size increases from 5.5
 322 nm at 25 mM to 10 nm at 60 mM (figure 5a). This increase in the apparent hydrodynamic
 323 size might either reflect a true increase in aggregate size, or it might indicate the existence
 324 of hydrodynamic interactions between complexes. Given that the ratio of SDS to GAD-
 325 2 molecules in a complex is not changing by much, i.e. $r \approx R$ (figure 5b), an increase in
 326 the mean aggregate size might arise from an increase in the average number of peptides
 327 in one complex from 1 (at 25 mM) to approximately 2 (at 60 mM). A third possibility is
 328 that such an increase in hydrodynamic radius arises from a change in shape (for example
 329 from spherical to oblate or prolate) (Bloomfield, 2000). However, in order to account for
 330 a factor two increase, one would need to have a rather spectacular shape change with
 331 a formation of very anisotropic complexes with an approximately 20:1 axial ratio. These
 332 three possibilities - an increase in number of peptides in a complex, long-range interactions
 333 between complexes, or a dramatic change in complex shape - are depicted in figure 7.
 334 As noted by (Zhou et al, 2008; Schreiber et al, 2009), a deeper understanding of role of
 335 electrostatic and hydrodynamic interactions is needed in the study of macromolecular
 336 crowding, and this needs to be studied further.

337 There is a distinct difference in the behavior of large peptides ($M_w^{\text{peptide}} > M_w^{\text{surfactant}}$) and
 338 small dipeptides ($M_w^{\text{peptide}} \approx M_w^{\text{surfactant}}$). The small dipeptides (Ala-Gly and Tyr-Leu) hardly

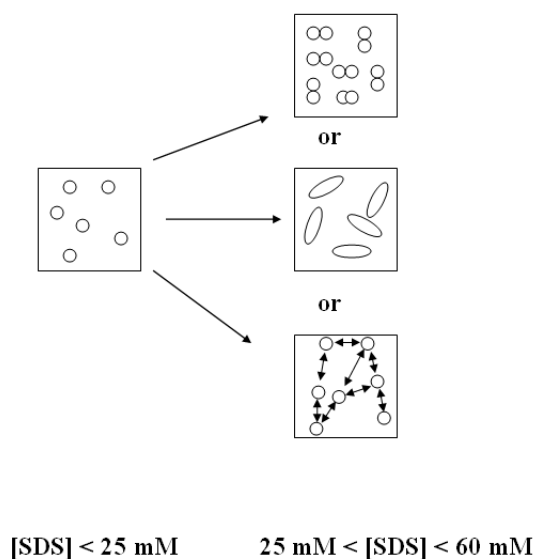


Fig. 7 A schematic diagram showing each peptide-surfactant complex as a single isolated complex (left, isolated circles) at low SDS concentrations. Results at intermediate SDS concentrations are consistent with either two peptides in each complex schematically represented by two circles (top right), highly anisotropic complexes (right middle), or long-range hydrodynamic interactions represented by arrows between complexes (right bottom).

339 affect the SDS diffusion coefficient (figure 6). This indicates that the dipeptides behave just
 340 as the surfactant does: i.e. rapidly exchanging between aggregate and free state. For large
 341 peptides such as GAD-2, on the other hand, rapid exchange between free and aggregate
 342 state is practically impossible. This is because the surfactant molecules form micellar-like
 343 aggregates along the peptide chain, consistent with a bead-on-a-chain picture (Chari et al,
 344 2004; Roscigno et al, 2003) for large-molecule aggregates. We therefore expect the approach
 345 outlined in this work to be valid generally for large hydrophobic peptides.

346 In conclusion, some recommendations are suggested in order to study peptides in
 347 membrane-mimic environments. All our results consistently show that measurements
 348 should be made in the regime where a two-species model is clearly valid, with the size
 349 of both free monomer and aggregate being independent of the surfactant concentration:
 350 this concentration is about 60 mM for pure SDS solutions. For peptide-SDS solutions, the
 351 true hydrodynamic size of the peptide-SDS complex is not necessarily constant even at
 352 intermediate concentrations less than 60 mM, and the concentration dependence of the hydro-

353 dynamic radius can still not be ignored. The only unambiguous concentration-independent
354 statements can be made at low concentrations: in this system, this is below [SDS]= 25 mM.

355 **4 Acknowledgments**

356 All the authors acknowledge financial support from the National Science and Engineering
357 Research Council of Canada (NSERC). We also acknowledge useful suggestions from Carl
358 Michal (University of British Columbia) and Ivan Saika-Voivod (Memorial University of
359 Newfoundland).

360 **References**

- 361 Altieri AS, Hinton DP, Byrd RA (1995) Association of biomolecular systems via pulsed field
362 gradient NMR self-diffusion measurements. *J Am Chem Soc* 117:7566–7561
- 363 Andersson A, Almqvist J, Hagn F, Maler L (2004) Diffusion and dynamics of penetratin in
364 different membrane mimicking media. *Biochim Biophys Acta* 61:18–25
- 365 Ando T, Skolnick J (2010) Crowding and hydrodynamic interactions likely dominate in
366 vivo macromolecular motion. *PNAS* 107:18,457–18,462
- 367 Barhoum S, Yethiraj A (2010) An NMR study of macromolecular aggregation in a model
368 polymer-surfactant solution. *J Chem Phys* 132:1–9
- 369 Batchelor GK (1976) Brownian diffusion of particles with hydrodynamic interaction. *J Fluid*
370 *Mech* 74:1–29
- 371 Begotka BA, Hunsader JL, Oparaeché C, Vincent JK, Morris KF (2006) A pulsed field
372 gradient NMR diffusion investigation of enkephalin peptide-sodium dodecyl sulfate
373 micelle association. *Magn Reson Chem* 44:586–593
- 374 Berr SS, Jones RRM (1988) Effect of added sodium and lithium chlorides on intermicellar
375 interactions and micellar size of aqueous dodecyl sulfate aggregates as determined by
376 small-angle neutron scattering. *Langmuir* 6:1247–1251
- 377 Binks BP, Chatenay D, Nicot C, Urbach W, Waks M (1989) Structural parameters of the
378 myelin transmembrane proteolipid in reverse micelles. *Biophys J* 55:949–955

- 379 Bloomfield VA (2000) Survey of Biomolecular Hydrodynamics. In: Separations and Hydro-
380 dynamics.(Todd M. Schuster, editor). On-Line Biophysics Textbook, Biophysics society,
381 www.biophysics.org
- 382 Browne MJ, Feng CY, Booth V, Rise ML (2011) Characterization and expression studies of
383 gaduscidin-1 and gaduscidin-2; paralogous antimicrobial peptide-like transcripts from
384 atlantic cod (*gadus morhua*). *Dev Comp Immunol* 35:399–408
- 385 Buchko GW, Rozek A, Hoyt DW, Cushley RJ, Kennedy MA (1998) The use of sodium dodecyl
386 sulfate to model the apolipoprotein environment. evidence for peptide SDS complexes
387 using pulsed-field-gradient NMR spectroscopy. *Biochim Biophys Acta* 1392:101–108
- 388 Chari K, Kowalczyk J, Lal J (2004) Conformation of poly(ethylene oxide) in polymer-
389 surfactant aggregates. *J Phys Chem B* 108:2857–2861
- 390 Chatterjee C, Majumder B, Mukhopadhyay C (2004) Pulsed-field gradient and saturation
391 transfer difference NMR study of enkephalins in the ganglioside GM1 micelle. *J Phys*
392 *Chem B* 108:7430–7436
- 393 Chen A, Wu D, Johnson CSJ (1995) Determination of the binding isotherm and size of the
394 bovine serum albumin-sodium dodecyl sulfate complex by diffusion-ordered 2D NMR.
395 *J Phys Chem* 99:828–834
- 396 Chinchar V, Bryan L, Silphadaung U, Noga E, Wade D, Rollins-Smith L (2004) Inactivation of
397 viruses infecting ectothermic animals by amphibian and piscine antimicrobial peptides.
398 *J Virol* 323:268–275
- 399 Cozzolino S, Sanna MG, Valentini M (2008) Probing interactions by means of pulsed field
400 gradient nuclear magnetic resonance spectroscopy. *Magn Reson Chem* 46:S16S23
- 401 Deaton KR, Feyen EA, Nkulabi HJ, Morris KF (2001) Pulsed-field gradient NMR study of
402 sodium dodecyl sulfate micelle-peptide association. *Magn Reson Chem* 39:276–282
- 403 Epand RM, Vogel HJ (1999) Diversity of antimicrobial peptides and their mechanisms of
404 action. *Biochim Biophys Acta* 1462:11–28
- 405 Fernandes JMO, Ruangsri J, Kiron V (2010) Atlantic cod piscidin and its diversification
406 through positive selection. *Public Library of Science* 5:1–7

- 407 Gao X, Wong TC (1998) Studies of the binding and structure of adrenocorticotropin peptides
408 in membrane mimics by NMR spectroscopy and pulsed-field gradient diffusion. *Biophys*
409 *J* 75:1871–1888
- 410 Gimel JC, Brown W (1996) A light scattering investigation of the sodium dodecyl sulfate-
411 lysozyme system. *J Chem Phys* 104:8112–8117
- 412 Hinton DP, Johnson CSJ (1994) Simultaneous measurement of vesicle diffusion coefficients
413 and trapping efficiencies by means of diffusion ordered 2D NMR spectroscopy. *Chem*
414 *Phys Lipids* 69:175–178
- 415 Hoskin DW, Ramamoorthy A (2008) Studies on anticancer activities of antimicrobial pep-
416 tides. *Biochim Biophys Acta* 1778:357–375
- 417 Iyota H, Krastev R (2009) Miscibility of sodium chloride and sodium dodecyl sulfate in the
418 adsorbed film and aggregate. *Colloid Polym Sci* 287:425–433
- 419 Jones JA, Wilkins DK, Smith LJ, Dobson CM (1997) Characterisation of protein unfolding
420 by NMR diffusion measurements. *J Biomol NMR* 10:199–203
- 421 Jones RAL (2002) *Soft Condensed Matter*, 1st edn. Oxford University Press Inc, New York
- 422 Morein S, Trouard TP, Hauksson JB, Rilfors U, Arvidson G, Lindblom G (1996) Two-
423 dimensional ^1H -NMR of transmembrane peptides from *escherichia coli* phosphatidyl-
424 glycerophosphate synthase in micelles. *Eur J Biochem* 241:489–497
- 425 Morns KF, Johnson CSJ (1993) Resolution of discrete and continuous molecular size distri-
426 butions by means of diffusion-ordered 2D NMR spectroscopy. *J Am Chem Soc* 115:4291–
427 4299
- 428 Morris KF, Johnson CSJ (1992) Diffusion-ordered two-dimensional nuclear magnetic reso-
429 nance spectroscopy. *J Am Chem Soc* 114:3139–3141
- 430 Morris KF, Froberg AL, Becker BA, Almeida VK, Tarus J, Larive CK (2005) Using NMR to
431 develop insights into electrokinetic chromatography. *Anal Chem* 77:254 A–263 A
- 432 Nicolas P (2009) Multifunctional host defense peptides: intracellular-targeting antimicrobial
433 peptides. *Federation of European Biochemical Societies* 276:6483–6496
- 434 Orfi L, Lin M, Larive CK (1998) Measurement of SDS micelle-peptide association using ^1H
435 NMR chemical shift analysis and pulsed-field gradient nmr spectroscopy. *J Anal Chem*

- 436 + 70:1339–1345
- 437 Price WS (1997) Pulsed-field gradient nuclear magnetic resonance as a tool for studying
438 translational diffusion: Part I. basic theory. *Concept Magnetic Res* 9:299–336
- 439 Qureshi T, Goto NK (2012) Contemporary methods in structure determination of membrane
440 proteins by solution NMR. *Top Curr Chem* 326:123–185
- 441 Rege K, Patel SJ, Megeed Z, Yarmush ML (2007) Amphipathic peptide-based fusion peptides
442 and immunoconjugates for the targeted ablation of prostate cancer cells. *Cancer Research*
443 *Journal* 67:6368–2375
- 444 Romani AP, Marquezina CA, Ito AS (2010) Fluorescence spectroscopy of small peptides
445 interacting with microheterogeneous micelles. *Int J Pharm* 383:154–156
- 446 Roscigno P, Asaro F, Pellizer G, Ortona O, Paduano L (2003) Complex formation between
447 poly(vinylpyrrolidone) and sodium decyl sulfate studied through NMR. *J Am Chem Soc*
448 119:9639–9644
- 449 Ruangsri J, Salger SA, Caipang CM, Kiron V, Fernandes JM (2012) Differential expression
450 and biological activity of two piscidin paralogues and a novel splice variant in atlantic
451 cod (*Gadus morhua* L.). *Fish Shellfish Immun* 32:396–406
- 452 Sammalkorpi M, Karttunen M, Haataja M (2009) Ionic surfactant aggregates in saline solu-
453 tions: Sodium dodecyl sulfate (SDS) in the presence of excess sodium chloride (NaCl) or
454 calcium chloride (CaCl₂). *J Phys Chem B* 113:5863–5870
- 455 Sanders CR, Sönnichsen F (2006) Solution NMR of membrane proteins: practice and chal-
456 lenges. *Magn Reson Chem* 44:s24–s40
- 457 Sarker M, Rose J, McDonald M, Morrow MR, Booth V (2011) Modifications to surfactant
458 protein b structure and lipid interactions under respiratory distress conditions: Conse-
459 quences of tryptophan oxidation. *J Biomol NMR* 50:25–36
- 460 Schreiber G, Haran G, Zhou HX (2009) Fundamental aspects of protein-protein association
461 kinetics. *Chem Rev* 109:839–860
- 462 Soderman O, Stilbs P (1994) NMR studies of complex surfactant systems. *Prog Nucl Mag*
463 *Res Sp* 26:445–482

- 464 Stilbs P (1982) Fourier transform NMR pulsed-gradient spin-echo (FT-PFGSE) self diffusion
465 measurements of solubilization equilibria in sds solutions. *J Colloid Interface Sci* 87:385–
466 394
- 467 Stilbs P (1983) A comparative study of micellar solubilization for combinations of sur-
468 factants and solubilizates using the fourier transform pulsed-gradient spin-echo NMR
469 multicomponent self-diffusion technique. *J Colloid Interface Sci* 94:463–469
- 470 Tulumello DV, Deber CM (2009) SDS micelles as a membrane-mimetic environment for
471 transmembrane segments. *J Biochem* 48:12,096–12,103
- 472 Wang G (1999) Structural biology of antimicrobial peptides by NMR spectroscopy. *Curr*
473 *Org Chem* 10:569–581
- 474 Wang G (2008) NMR studies of a model antimicrobial peptide in the micelles of SDS, dode-
475 cylphosphocholine, or dioctanoylphosphatidylglycerol. *The Open Magnetic Resonance*
476 *Journal* 1:9–15
- 477 Whitehead TL, Jones LM, Hicks RP (2001) Effects of the incorporation of CHAPS into
478 SDS micelles on neuropeptide-micelle binding: Separation of the role of electrostatic
479 interactions from hydrophobic interactions. *Biopolymers* 58:593–605
- 480 Whitehead TL, Jones LM, Hicks RP (2004) PFG-NMR investigations of the binding of
481 cationic neuropeptides to anionic and zwitterionic micelles. *J Biomol Struct Dyn* 21:567–
482 576
- 483 Wu D, Chen A, Johnson CS (1994) An improved diffusion ordered-spectroscopy experiment
484 incorporating bipolar-gradient pulses. *J Magn Reson Ser A* 115:260–264
- 485 Yu L, Tan M, Ho B, Ding JL, Wohland T (2006) Determination of critical micelle concentra-
486 tions and aggregation numbers by fluorescence correlation spectroscopy: Aggregation of
487 a lipopolysaccharide. *Anal Chim Acta* 556:216–225
- 488 Zasloff M (2002) Antimicrobial peptides of multicellular organisms. *Nature* 415:389–395
- 489 Zhou HX, Rivas G, , Minton AP (2008) Macromolecular crowding and confinement: bio-
490 chemical, biophysical, and potential physiological consequences. *Annu Rev Biophys*
491 37:375–397